Velocity Profiles of Thoria Suspensions in Turbulent Pipe Flow

D. M. EISSENBERG and D. C. BOGUE

Oak Ridge National Laboratory, Oak Ridge, Tennessee

Velocity profiles and friction factors of non-Newtonian fluids in turbulent pipe flow can be displayed with the semiempirical forms developed for Newtonian fluids in which the apparent viscosity evaluated at the wall shear stress is used.

Friction factors and velocity profiles were obtained for a dilute and a concentration aqueous thoria suspension and compared with the Newtonian correlations and with previous data obtained from widely different non-Newtonian fluids including a viscoelastic fluid. A relationship is shown between the decrease of the friction factor and the change in the velocity distribution towards a more laminar profile.

A generalized method of deriving the friction factor-Reynolds number plot from the velocity profile based on the von Kármán relationship for Newtonian fluids is derived and compared with the data.

BACKGROUND

Turbulent Newtonian velocity profiles have been correlated in a variety of semiempirical forms, the most common one involving the dimensionless parameters u^+ and $\log y^+$. Such a form, while convenient, is not accurate in complete detail, the experimental deviations from it being primarily a function of dimensionless radial position y/R. A review of corrections to the $u^+ - y^+$ form has been made and a new empirical correction term devised (*1*). The final result for the turbulent core is of the form

$$u^+ - c = 5.57 \log y^+ + 5.57 \qquad (1)$$

where $c = c(y/R, f)$, a small empirical correction term, is given by

$$c(y/R, f) = 0.05 \sqrt{2/f} \exp \frac{-(y/R - 0.8)^2}{0.15} \qquad (2)$$

Equation (1) can be rearranged into the form

$$\frac{u_{\max} - u}{u^*} = 5.57 \log (y/R) + [c(1, f) - c(y/R, f)] \qquad (3)$$

where the term on the left is known as the *velocity defect.* When one assumes that the flow is essentially all in the turbulent core, Equation (1) can be integrated across the pipe to yield the classical von Karman friction factor-Reynolds number correlation (*1*).

Equations (1) and (3), being applicable to all Newtonian fluids, provide a useful basis for comparing Newtonian and non-Newtonian velocity profiles. In the case of Equation (1) (and also for any friction factor correlations which may be devised) one must choose an appropriate non-Newtonian viscosity or a non-Newtonian Reynolds number. For convenience in displaying and using friction factor data a Reynolds number which is natural in laminar flow can be extended empirically into the turbulent flow regime (*4*). For mechanistic purposes however it is more helpful to use the apparent viscosity evaluated at the wall shear stress (*1, 2, 3*), the motivation being that the viscous effects in the wall region are the most important viscous effects which occur in the pipe. This apparent viscosity, calculated by assuming the existence of a laminar sublayer sufficiently close to the pipe wall, is obtained by dividing the wall shear stress, as calculated from pressure drop data, by the laminar shear rate, as obtained from a laminar shear diagram:

$$\mu_w = \left(\frac{\tau_{rz}}{du/dr} \right)_{\text{wall}} \qquad (4)$$

The use of this viscosity has been found to reduce to a considerable extent the dependence of the correlations on arbitrary parameters based on rheological models, although for prediction purposes it is more difficult to use in that a trial-and-error technique is necessary if the viscosity is changing rapidly in the shear stress range of interest.

Three previous studies involving the measurements of velocity profiles in non-Newtonian fluids have been carried out (*1, 5, 6*). The fluids used included pseudoplastic aqueous solutions of carboxypolymethylene (Carbopol), carboxymethylcellulose (CMC), and ammonium alginate (alginate), and aqueous suspensions of clay (Attagel). The CMC solution is known to exhibit viscoelastic behavior in the sense that it exhibits normal stress and birefringence effects under shear (*7, 8*).

The first measurements of velocity profiles were made by Shaver (*5*) using CMC and alginate. He presented the data graphically in the form of the velocity defect equation using as a parameter the non-Newtonian flow behavior index (n) of the power law rheological model. Shaver's results (Figure 1) showed a progressive change in the turbulent velocity profile toward a less blunt (more laminar) velocity profile with decreasing values of the rheological constant n. In addition to profiles Shaver obtained friction factors over a range of mean velocities. These results have been replotted in Figure 2 against the Reynolds number based upon the wall shear stress viscosity. It is noted that the friction factors lie well below the Newtonian line.

Bogue (*1*) measured the velocity profile and friction factor in turbulent pipe flow of Carbopol and Attagel, neither of which is known to be strongly viscoelastic, although it is understood that dynamic and normal stress measurements on Carbopol have recently been made (*9*). After considering the scatter in all of his data, he concluded there were no significant differences between the Newtonian and non-Newtonian velocity profiles. At the lowest values of n however there is some suggestion that the velocity defect near the wall might be larger for the non-Newtonian fluids, in qualitative but not quantitative agreement with Shaver's results. The range of Bogue's data is indicated in Figure 1; the power law index n ranged between 0.46 and 1.0. Friction factors for Carbopol and Attagel, obtained by Bogue and by Dodge (*4*) for this range of n, are included in Figure 2.

D. C. Bogue is at the University of Tennessee, Knoxville, Tennessee.

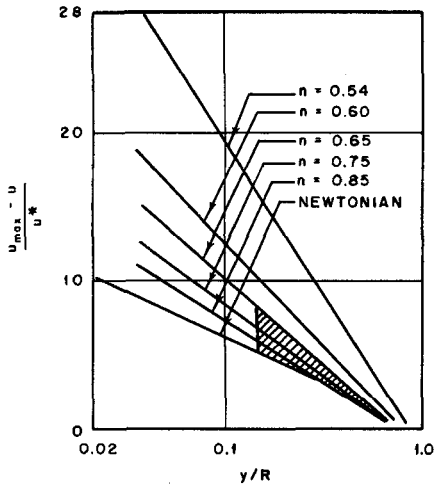

Fig. 1. Velocity profile data of Shaver. (Data of Bogue for $n = 0.45$ to 0.54 shown as hatched area.)

The third set of measurements of velocity profiles was carried out by Clapp (6) using Carbopol with $n > 0.7$. The velocity profiles, as expressed in the form of Equation (1), were Newtonian. The friction factors agreed with those of Dodge and of Bogue for that value of n.

A comparison of the data of Shaver with that of Bogue and of Clapp suggests that the effect of a viscoelastic material was to alter the turbulent flow behavior (as measured both by the friction factor depression for a given Reynolds number and by the velocity defect change) by a greater amount than does a nonelastic material with the same non-Newtonian flow behavior index. This tendency of the viscoelastic flow to be more nearly laminar is qualitatively reasonable if one argues that the long polymer molecules elongate themselves in the direction of flow, thereby offering increased resistance to turbulent fluctuations in the transverse direction.

It was the purpose of the work reported here to measure velocity profiles and friction factors for a non-Newtonian slurry, a suspension of thoria in water. The work is reported in detail in a thesis (2). The friction factor data are presented with only brief comment, since more extensive friction factor data for high temperature thoria slurries has been discussed more fully elsewhere (3).

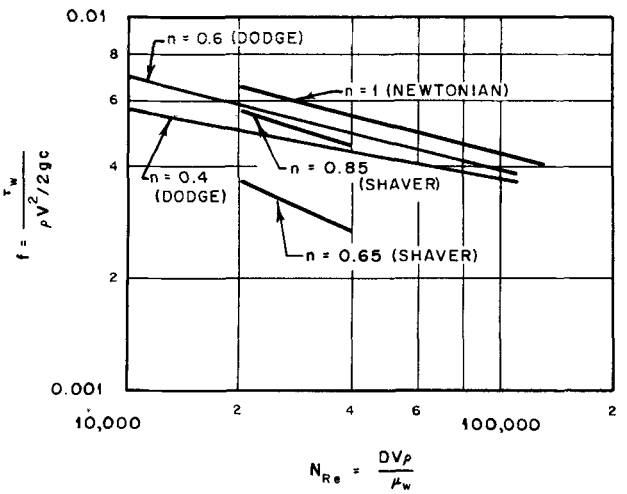

Fig. 2. Recalculated friction factor data of Shaver and Dodge plotted using Reynolds number based on wall shear viscosity.

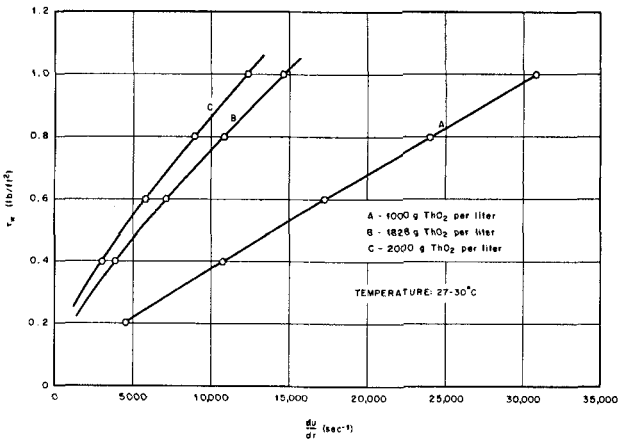

Fig. 3. Thoria suspension shear diagrams.

PROPERTIES OF THORIA SLURRIES

The thoria slurries used consist of suspensions of microscopic particles of thoria of random granular shape with edges rounded as a result of high-temperature pumping. They have an equivalent particle diameter of about 1μ. The suspensions are colloidally unstable tending to form loose visible flocs (or clusters of particles) on the order of one half millimeter diameter which maintain their identity under mild agitation.

The slurries are shear thinning; that is the viscosity decreases with increasing shear stress. There is no qualitative evidence of viscoelastic behavior. Shear diagrams for the suspensions used in the experiment, which are shown in Figure 3, were obtained from data taken with a 0.018-in. I.D. vertical capillary tube viscometer. Since the shear diagrams include data for high shear stresses, it was not necessary to extrapolate the curves by means of a rheological equation to obtain the wall shear stress viscosity. For that reason no rheological model was chosen to represent the data.

EXPERIMENTAL

The experiments were carried out in a circulating slurry loop (Figure 4) which had previously been constructed and utilized for heat transfer measurements. The loop was fabricated of 1½ and 2 in. galvanized steel pipe. A positive displacement pump provided the flow and was driven by an electric motor through a variable speed drive. The maximum flow rate used in the experiment was 95 gal./min.

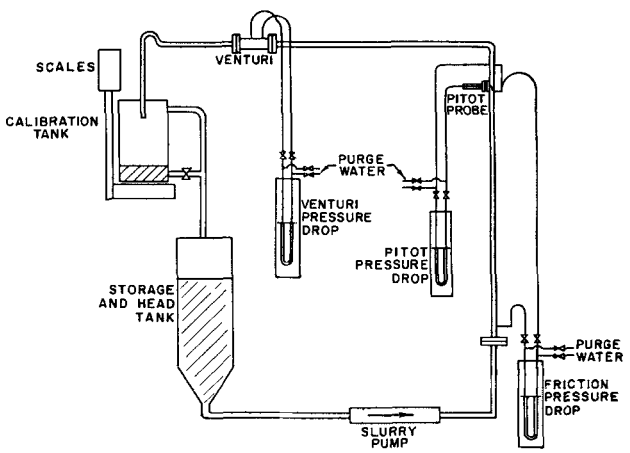

Fig. 4. Schematic of experimental loop.

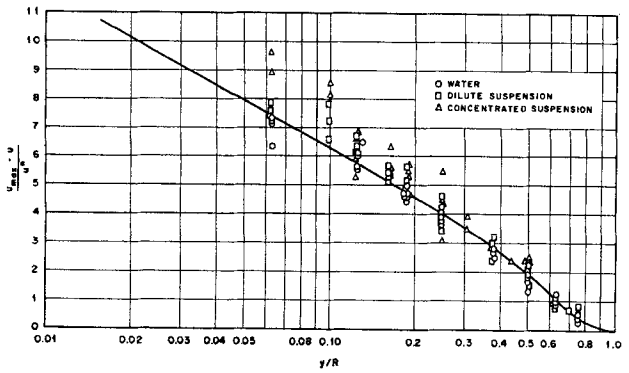

Fig. 5. Velocity defect plot of data.

An open tank of approximately 100 gal. capacity provided 4 ft. of suction head for the pump. The tank was equipped with a propeller type of stirrer. A second open storage tank which was part of the circulation loop drained into the head tank from an overhead platform. This tank was mounted on calibrated weighing scales and was equipped with a quick opening valve in the bottom drain, and an overflow drain. It was used to calibrate the loop Venturi meter.

A 15-ft. vertical run of loop piping fabricated of commercial smooth brass pipe of 1.60-in. I.D. constituted the test section. It contained a 2-ft. straightening vane at the bottom (upstream) end. The upstream wall static pressure tap was located 2 ft. downstream from the straightening vane. The downstream wall static tap was located 119 in. above the upstream tap. Both taps were ⅛-in. I.D.

A Venturi was located in a section of horizontal 2-in. I.D. loop piping downstream of the test section. The Venturi throat diameter was 0.8625 in.

The velocity probe assembly consisted of a traversing impact tube with a shank of ⅛-in. O.D. The tube tip facing upstream was ¾ in. long and was made of hypodermic tubing of 0.066-in. O.D. and 0.047-in. I.D. The probe was inserted into the loop through a ½-in. access hole and was positioned within the pipe with a vernier positioner.

The downstream static pressure tap was used in conjunction with the impact tube. It was located at the same axial position as the impact tube tip and displaced 90 deg. from the access hole.

Whereas the impact probe correctly reads the total impact plus static pressure, the wall static pressure reading has a small error due to the presence of a velocity gradient at the wall. An empirical velocity correction factor, applicable for water in a large range of pipe sizes, has been reported to be a function of the pipe factor, defined as the ratio of the mean velocity to the center-line velocity (*11*). For the water data taken in this experiment the pipe factor is of the order of 0.8 to 0.85, and the correction factor is 0.975. Because this correction factor cannot be assumed to apply to non-Newtonian fluids, and because it is of such small magnitude, it was not applied to any of the present data.

Three U-tube manometers were used in the experiment. They were connected to the pressure taps with tubing which had been looped 1 ft. above each pressure tap before being connected. This provided a visual means of determining whether thoria suspension was in the tubing. A water line was connected with a separate valve to each leg of each manometer so that water could be flushed through the tubing lines to the loop to purge any thoria prior to obtaining readings.

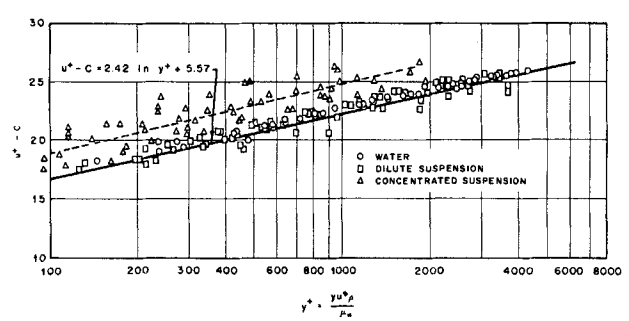

Fig. 6. Modified $u^+ - y^+$ plot based on wall shear viscosity.

VISCOMETER

An existing vertically oriented capillary tube viscometer (*12*) was utilized to obtain laminar flow shear diagrams. The viscometer consisted of a 0.01805-in. I.D. stainless steel capillary encased for rigidity in a ¼-in. O.D. steel tube. It was connected on the bottom to a 250-ml. stirred pressurized autoclave. The top of the capillary was connected to a volume-calibrated cylindrical sight glass. Pressure was supplied by the building air supply and was measured with a 75-in. mercury manometer.

The viscometer tube had been calibrated with water and glycerol during previous experiments. Corrections for static head and for kinetic energy loss (Hagenbach correction) were made for all calibrations and all viscometry.

RESULTS

Five complete profiles and several additional center-line velocities, were obtained with water over a range of mean velocities. Friction pressure drops were obtained for each mean velocity. The results are summarized in the form of a velocity defect plot, Figure 5, a $u^+ - y^+$ diagram, Figure 6, and a friction factor—Reynolds number plot, Figure 7. The velocity defect data are compared with Equation (3), in which the correction terms were evaluated at a friction factor of 0.0045. A single comparison line was used, since the correction terms were insensitive to friction factors in the range of this experiment (± 25% of 0.0045). The $u^+ - y^+$ data were not plotted directly, the calculated u^+ being modified by subtracting the correction term in Equation (1) before plotting. Since the correction term represents the difference between the actual u^+ and the u^+ predicted by the semilogarithmic correlation, the result of applying the correction term before plotting is to line up all the Newtonian data on a single $u^+ - y^+$ line. The use of this correction term with the non-Newtonian data is an arbitrary one, but it was used so that the resulting modified $u^+ - y^+$ diagrams could be compared on an equal basis with the literature data.

The suspension profile data consist of eleven profiles at two concentrations of thoria (800 to 1,000 and 1,700 to 2,000 g. thoria/liter). In addition a number of center-line velocities were obtained at the higher concentration. Friction factors were obtained for each mean velocity. The results are also plotted as velocity defects, modified $u^+ - y^+$ diagrams, and friction factors. The center-line velocities obtained are also included in the modified $u^+ - y^+$ diagrams. For the $u^+ - y^+$ diagrams and for the friction factor correlation the value of the viscosity was evaluated from the shear diagrams (Figure 3) at the wall shear stress which existed during the experiments.

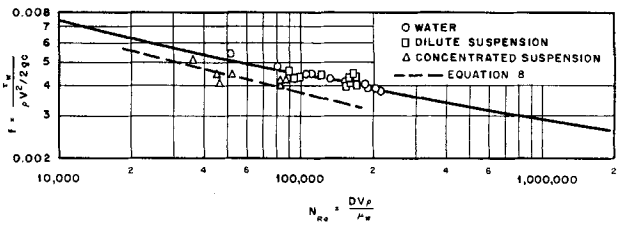

Fig. 7 Friction factor vs. Reynolds number based on wall shear viscosity.

Examination of Figure 7 shows that the dilute slurry and the water friction factors fall along the smooth tube line for Newtonian fluids, whereas the concentrated slurry friction factors are about 15% lower. The modified $u^+ - y^+$ data for both water and dilute slurry (Figure 6) lie parallel to and about 2% above the predicted Newtonian line. If the correction factor (*11*) for the static tap noted earlier were applied, the data would coincide with the predicted line. The velocity defect representation of the data for the fluids showed no apparent deviation from the Newtonian line.

Both the modified $u^+ - y^+$ and the velocity defect representation of the concentrated slurry velocity profile data lie above the Newtonian line by about 20%. The scatter appearing in the $u^+ - y^+$ and velocity defect representations of the velocity profiles of the concentrated slurry is related to the scatter of the friction factor data in that the lowest friction factors coincide with the highest velocity defect and u^+ points.

DISCUSSION

The velocity profiles and friction factors obtained with the dilute thoria slurry follow the Newtonian correlations closely, providing the viscosity of the slurry used in the Reynolds number and in y^+ is evaluated at the wall shear stress. This result for the friction factors is in agreement with that obtained with similar dilute slurries at temperatures up to 200°C. (*3*).

The friction factors for the concentrated slurry were lower than Newtonian, also in agreement with previous results with concentrated thoria slurries (*3*) and with other non-Newtonian fluids (*1*). When the velocity profiles of this suspension are displayed as velocity defect plots and as modified $u^+ - y^+$ diagrams, the profiles are somewhat steeper and the u^+ intercepts (at $y^+ = 1$) somewhat larger than the Newtonian correlation. These results, for both dilute and concentrated slurry, are in qualitative agreement with the data of Shaver and of Bogue.

There is in addition an interesting similarity between these literature results and the present work. It is noted from Figures 2 and 7 that the concentrated thoria slurry friction factors lie along a line corresponding to a flow behavior index of 0.85 as obtained by Shaver. When the predicted velocity profile for $n = 0.85$ (Figure 1) is compared with Figure 5, it is seen that they also coincide for the concentrated slurry. In other words one can associate the lower friction factors with a change in the shape of the velocity profile. This change occurs throughout the pipe rather than being restricted to the viscosity-dominated region near the pipe wall.

Friction factor data alone can never lead to a prediction of velocity profiles (the former being an integrated property of the latter), although the accumulated experience cited above suggests that if one observes lower-than-Newtonian friction factors (judged on a plot of f vs. $DV\rho/u_w$), one can expect sharper (more laminarlike) velocity profiles. The reverse problem, that of going from velocity profiles to friction factors, is simply one of mathematics, the velocity profile correlations themselves containing a shear stress parameter in the form of u^* ($\equiv \sqrt{f/2}\, V$). Any set of equations which fit the velocity profile data can be integrated to give a friction factor prediction. A straightforward approach is that due basically to von Kármán, as quoted in Knudsen and Katz (*13*). One starts with the velocity profile equation for the wall region, Equation (4), rewritten as

$$u^+ = y^+ \tag{5}$$

and the equation for the turbulent core

$$\frac{u_{max} - u}{u^*} = -\frac{1}{K_p} \ln (y/R) \tag{6}$$

One now assumes that the two equations can be fitted at the transition boundary given by

$$u^+_\delta = y^+_\delta = \text{constant for a given fluid}$$

In essence the equations give a two parameter fit with K_p and u^+_δ (or y^+_δ) as the adjustable constants. Rearranging Equation (6) one gets

$$u^+ = \frac{1}{K_p} \ln y^+ + \left(u^+_\delta - \frac{1}{K_p} \ln y^+_\delta \right) \tag{7}$$

The values of K_p and u_δ obtained from the data in Figure 6 are

	Newtonian and dilute slurry data	Concentrated slurry data
K_p	0.413	0.373
u^+_δ ($= y^+_\delta$)	11.5	13.4

If Equation (7) is integrated across the pipe, the result is

$$\frac{1}{\sqrt{f}} = \frac{0.707}{K_p} \ln \left(N_{Re} \sqrt{f} + 0.707 \left[u^+_\delta - \frac{1}{K_p} \ln u^+_\delta - \frac{2.54}{K_p} \right] \right) \tag{8}$$

Inserting the concentrated parameters into Equation (8) yields the dotted line shown in Figure 7. The agreement with the experimental data demonstrates the internal consistency of the correlations and strengthens one's confidence in the accuracy of the observed differences from Newtonian behavior.

In comparing bluntness or sharpness of various velocity profiles one must recognize the arbitrariness in the selection of parameters. The use of u^* in normalizing velocity data introduces the friction factor (or shear stress) into the correlation, whether one identifies it explicitly or not. An alternate normalizing parameter is the mean velocity V (see for example *1*). If one plots the non-Newtonian data in the form of $(u_{max} - u)/V$ vs. y/R, the profiles are nearly Newtonian, although they still show a deviation in the direction of a steeper profile. Such plots would suggest more of a viscosity effect in the wall region. Physically however it would appear more rational to use u^*, since the generation of turbulence is surely related to the stress and not just to the mean velocity.

CONCLUSIONS

The velocity profiles in turbulent pipe flow of a dilute non-Newtonian suspension of thoria in water, one for which the friction factors in turbulent flow follow the Newtonian correlations, were found to follow the Newtonian profile when displayed as velocity defect plots and as $u^+ - y^+$ diagrams. The viscosity used in the Reynolds number and in y^+ was the experimentally determined wall shear stress viscosity.

For concentrated suspensions, for which the friction factors in turbulent flow were lower than the Newtonian correlation, the velocity profiles were somewhat steeper than their Newtonian counterparts.

The results are in qualitative agreement with available slurry and dilute polymer data including those for viscoelastic fluids. A comparison of these data with the present results suggests that a given friction factor decrease in turbulent flow for either an elastic or an inelastic fluid is associated with roughly the same velocity profile, in spite of diversity of mechanisms responsible for the non-Newtonian flow characteristics of these types of fluids.

The friction factor and velocity profile data are internally consistent, as evidenced by treatment with an extension of the von Kármán correlating equation.

NOTATION

c = empirical correction term, Equation (2)
D = pipe diameter, ft.
f = $\dfrac{\tau_w}{\rho V^2/2g_c}$, friction factor
n = parameter in the power law model, $\tau_{rz} = K\left(-\dfrac{du}{dr}\right)^n$
N_{Re} = $\dfrac{DV\rho}{u_w}$, Reynolds number
r = radial position, ft.
R = pipe radius, ft.
u = mean point velocity in pipe, ft./sec.
u^+ = u/u^*, dimensionless velocity
u^* = $\sqrt{\tau_w g_c/\rho}$, friction velocity, ft./sec.
u_{max} = center-line velocity, ft./sec.
V = mean velocity, ft./sec.
y = distance from wall, ft.
y^+ = $\dfrac{y\,u^*\,\rho}{\mu_w}$, dimensionless distance
ρ = density, lb.$_m$/cu. ft.
μ_w = apparent viscosity, Equation (4), lb.$_m$/(sec.)(ft.) (= μ, Newtonian fluids)
τ_w = shear stress at the wall, lb.$_f$/sq. ft.
τ_{rz} = shear stress in general, lb.$_f$/sq. ft.

LITERATURE CITED

1. Bogue, D. C., and A. B. Metzner, *Ind. Eng. Chem. Fundamentals*, **2**, 143 (1963).
2. Eissenberg, D. M., M.S. thesis, University of Tennessee, Knoxville, Tennessee (1963).
3. ———, *A.I.Ch.E. Journal*, **10**, 403 (May, 1964).
4. Dodge, D. W., and A. B. Metzner, *ibid.*, **5**, 189 (1959).
5. Shaver, R. G., and E. W. Merrill, *ibid.*, p. 181.
6. Clapp, R. M., in "International Developments in Heat Transfer, Part III," *Am. Soc. Mech. Engrs.*, New York (1961).
7. Metzner, A. B., W. T. Houghton, R. A. Sailor, and J. L. White, *Trans. Soc. Rheo.*, **5**, 133 (1961).
8. Brodnyan, J. G., F. H. Gaskins, and W. Philippoff, *ibid.*, **2**, 285 (1958).
9. Meter, D. M., Ph.D. thesis, University of Wisconsin, Madison, Wisconsin (1963).
10. Bogue, D. C., Ph.D. thesis, University of Delaware, Newark, Delaware (1960).
11. Hubbard, C. W., *Trans. Am. Soc. Mech. Engrs.*, **61**, 477 (1939).
12. Eissenberg, D. M., *U.S.A.E.C. ORNL 3233* (Feb. 28, 1962).
13. Knudsen, J. G., and D. L. Katz, "Fluid Dynamics and Heat Transfer," p. 172, McGraw-Hill, New York (1958).

Manuscript received February 10, 1964; revision received April 6, 1964; paper accepted April 7, 1964. Paper presented at A.I.Ch.E. Houston meeting.

An Ionic Penetration Theory for Mass Transfer With Chemical Reaction

P. L. T. BRIAN, R. F. BADDOUR, and D. C. MATIATOS

Massachusetts Institute of Technology, Cambridge, Massachusetts

Theoretical analyses based upon film theory and penetration theory models of the interphase mass transfer process have contributed greatly to the understanding of the effect of a simultaneous chemical reaction upon the rate of mass transfer. For a review of these and other models and their use in predicting the effect of a chemical reaction upon the mass transfer rate the reader is referred to references 2, 3, 4, 5, 6, 7, 19, and 22. An especially interesting aspect of these theoretical studies has been the surprising agreement of film theory predictions with penetration theory predictions except when diffusivity ratios depart greatly from unity (3, 6).

Most of the theoretical treatments of simultaneous mass transfer and chemical reaction have been based on the assumption that the various diffusing and reacting species were uncharged molecules, although in most commercially important examples of simultaneous mass transfer and chemical reaction ionic species are involved. Furthermore it has long been known (14, 15, 17, 18) that ions, since they are electrically charged, obey a different law of diffusion than that for molecular species. This lead Sherwood and Wei (21) and later Sherwood and Ryan (20) to a study of ion diffusion effects upon the film theory solution for mass transfer accompanied by an infinitely rapid irreversible chemical reaction. Sherwood and Wei showed that ion diffusion effects were large in the systems they studied and also that their diffusion cell data for these systems supported their ionic theory.